

Discrete solitons in self-defocusing systems with \mathcal{PT} -symmetric defects

Zhiqiang Chen¹, Jiasheng Huang¹, Jinglei Chai¹, Xiangyu Zhang^{1,2}, Yongyao Li^{1,*} and Boris A. Malomed³

¹*Department of Applied Physics, South China Agricultural University, Guangzhou 510642, China*

²*Department of Electrical and Computer Engineering,
Duke University, Durham, North Carolina 27708, USA*

³*Department of Physical Electronics, School of Electrical Engineering,
Faculty of Engineering, Tel Aviv University, Tel Aviv 69978, Israel.*

We construct families of discrete solitons (DSs) in an array of self-defocusing waveguides with an embedded \mathcal{PT} (parity-time)-symmetric dimer, which is represented by a pair of waveguides carrying mutually balanced gain and loss. Four types of states attached to the embedded defect are found, namely, staggered and unstaggered bright localized modes and gray or anti-gray DSs. Their existence and stability regions expand with the increase of the strength of the coupling between the dimer-forming sites. The existence of the gray and staggered bright DSs is qualitatively explained by dint of the continuum limit. All the gray and anti-gray DSs are stable (some of them are unstable if the dimer carries the *nonlinear* \mathcal{PT} symmetry, represented by balanced nonlinear gain and loss; in that case, the instability does not lead to a blowup, but rather creates oscillatory dynamical states). The boundary between the gray and anti-gray DSs is predicted in an approximate analytical form.

PACS numbers: 42.65.Tg; 42.70.Qs; 05.45.Yv

I. INTRODUCTION

Dynamics of discrete systems has been a subject of intensive studies in diverse areas of physics, including dynamical lattices and long molecules, optics, ultracold atomic gases, lattice QCD, etc. [1]-[22]. In particular, it is well established that optical discrete solitons (DSs) readily self-trap in nonlinear waveguiding arrays [8, 13]. In addition to their significance to fundamental studies, DSs offer various possibilities for all-optical data-processing applications; in particular, they can implement intelligent functional operations, such as routing, blocking, logic functions and time-gating [23]. Therefore, methods allowing one to control the formation, mobility and interactions of DSs have been a subject of many theoretical and experimental studies.

It is well known too that light confinement can be realized with the help of various defects. Linear photonic defects can be created as localized structures in photonic crystals [24], nanocavities [25], microresonators [26] and quantum-dot settings [27]. In particular, defects have been designed to control DSs in arrayed waveguides [28]-[33]. Nonlinear defects in photonic arrays have also been elaborated, chiefly theoretically [34]-[42].

Recently, attention has been drawn to defects formed by parity-time (\mathcal{PT})-symmetric dimers, i.e., pairs of cores carrying mutually balanced gain and loss, embedded into waveguide arrays [42-44] (related settings are represented by gain cores embedded into dissipative lattices [46]-[48]), as well as continuum counterparts of such systems, with the embedded dimer (alias a \mathcal{PT} -symmetric dipole) represented by a combination of the delta function and its derivative, in the real and imaginary parts, respectively [49]. These lattice systems, which are governed by discrete nonlinear Schrödinger (DNLS) equations corresponding to \mathcal{PT} -symmetric non-Hermitian Hamiltonians [4], [50]-[56], give rise to entirely real propagation spectra, provided that the strength of the gain and loss terms does not exceed a critical level, past which the \mathcal{PT} symmetry suffers spontaneous breaking (a possibility of having *unbreakable* \mathcal{PT} symmetry was recently reported in a model incorporating self-defocusing nonlinearity with the local strength growing fast enough from the center to periphery [56]). Linear \mathcal{PT} systems were realized experimentally in optics, by coupling pumped and lossy waveguides [58]-[60]. The simplest version of \mathcal{PT} -symmetric nonlinear systems was elaborated theoretically in the form of dimers with the onsite Kerr [61]-[64] or quadratic [65] terms. A *nonlinear* version of the \mathcal{PT} symmetry, represented by the balanced nonlinear gain and loss, was introduced too [42, 66].

Previous works on \mathcal{PT} -symmetric dimers embedded into lattices were dealing with the self-focusing nonlinearity or linear lattices [42-44], while self-defocusing is also possible in photonics [13, 67]. In this work, we introduce the system with a \mathcal{PT} -symmetric dimer embedded into a one-dimensional array of self-defocusing waveguides. The system is described by a DNLS equation with a defect representing the dimer. As a generalization, we also briefly consider the dimer with the nonlinear \mathcal{PT} symmetry. We find that the system supports stable staggered and unstaggered localized

*Electronic address: yongyaoli@gmail.com

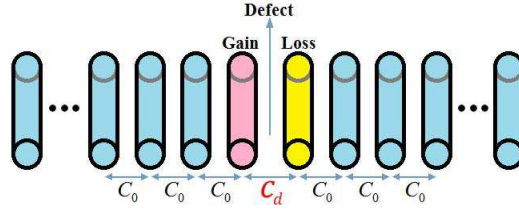


FIG. 1: (Color online) The schematic of the nonlinear waveguide array with the defect represented by the embedded \mathcal{PT} -symmetric dimer.

modes (bright DSs pinned to the defect), along with gray and anti-gray DSs (the latter means a soliton featuring a local elevation on top of a flat background [14]). Existence regions for them are found in a partly analytical form, using the continuum limit of the discrete systems. The stability of the DSs is investigated by means of numerical methods, *viz.*, calculation of eigenvalues for small perturbations, and direct simulations of the underlying DNLS equation.

The paper is structured as follows. The models are introduced in section II. Bright DSs (staggered and unstaggered ones) and gray and anti-gray DSs are studied, respectively, in section III and IV (the latter section also includes the consideration of DSs pinned to the defect with the nonlinear \mathcal{PT} symmetry). The paper is concluded by section VI.

II. THE MODELS

A. The system with the linear \mathcal{PT} symmetry

The lattice system with the defect carrying the linear \mathcal{PT} symmetry is based on the DNLS equation written as

$$i \frac{du_n}{dz} = -(C_{n-1,n}u_{n-1} + C_{n,n+1}u_{n+1}) + |u_n|^2u_n + i\kappa_n u_n, \quad (1)$$

where u_n is the amplitude of light in the n -th core of the arrayed waveguide, z is the propagation distance, $C_{n,n+1}$ and κ_n are the coupling constant and gain-loss coefficient, respectively. As said above, the array features the self-defocusing on-site nonlinearity and an embedded defect, which is formed by the pair of sites with a tunable strength, C_d , of the coupling between them, see Fig. 1. The two defect-forming sites carry mutually balanced linear gain and loss, which is described by κ and $-\kappa$ ($\kappa > 0$).

Thus, coefficients $C_{n,n+1}$ and κ_n in Eq. (1) are defined as

$$C_{n,n+1} = \begin{cases} C_d & \text{at } n = -1, \\ C_0 & \text{at } n \neq -1, \end{cases} \quad \kappa_n = \begin{cases} \kappa & \text{at } n = -1, \\ -\kappa & \text{at } n = 0, \\ 0 & \text{elsewhere,} \end{cases} \quad (2)$$

where C_0 is the inter-site coupling constant outside of the defect, and N is the size of the array. It is implied that $C_d/C_0 > 1$ and $C_d/C_0 < 1$ correspond to the distance between the defect-forming sites which is, respectively, smaller or larger than the separation between the sites outside of the defect. Propagating modes are characterized by the total field power (alias norm of the solution),

$$P = \sum_{n=-N/2}^{N/2-1} |u_n|^2. \quad (3)$$

Hereafter, we fix $C_0 = 1/2$ by means of obvious rescaling, and produce numerical results for the system of size $N = 128$, with P , C_d and κ treated as control parameters.

Stationary solutions to Eq. (1) with real propagation constant $-\mu$ are looked for as

$$u_n(z) = U_n e^{-i\mu z}, \quad (4)$$

where U_n is the distribution of the local amplitudes. Stationary solutions were found in the numerical form by means of the imaginary-time-propagation method [68], while real-time simulations of Eq. (1) were carried out using the four-step Runge-Kutta algorithm with the periodic boundary conditions.

Stability of the localized stationary modes was investigated numerically by means of computing eigenvalues for small perturbations, and the results were verified by means of direct simulations of the perturbed evolution in the framework of Eq. (1). The perturbed solution was taken as

$$u_n = e^{-i\mu z} (U_n + w_n e^{i\lambda z} + v_n^* e^{-i\lambda^* z}),$$

where the asterisk stands for the complex conjugate. The substitution of this expression into Eq. (1) and linearization leads to the eigenvalue problem for the perturbation wavenumber, $\lambda \equiv \lambda_r + i\lambda_i$, and the eigenmodes, $\{w_n, v_n\}$:

$$\begin{pmatrix} C - \mu + 2|U_n|^2 + i\kappa_n & U_n^2 \\ - (U_n^*)^2 & -C + \mu - 2|U_n|^2 + i\kappa_n \end{pmatrix} \begin{pmatrix} w \\ v \end{pmatrix} = \lambda \begin{pmatrix} w \\ v \end{pmatrix}. \quad (5)$$

Solution U_n is stable if all eigenvalues λ are real.

B. Generalization for the nonlinear \mathcal{PT} symmetry

The lattice with the embedded dimer featuring the nonlinear \mathcal{PT} symmetry is described by the following version of the DNLS equation:

$$i \frac{du_n}{dz} = - (C_{n-1,n} u_{n-1} + C_{n,n+1} u_{n+1}) + (1 + i\kappa_n) |u_n|^2 u_n, \quad (6)$$

where coefficients C_n and κ_n are again defined as per Eqs. (2). In terms of the optical realization, the nonlinear gain may be provided by a combination of the usual linear amplification and saturable absorption, while the nonlinear loss is usually induced by resonant two-photon absorption [67, 69]. A more general system, including linear and nonlinear \mathcal{PT} -symmetric terms, is possible too [42], but the corresponding analysis is rather cumbersome.

III. BRIGHT MODES

A. Staggered bright discrete solitons

The standard staggering transformation is introduced by replacing the lattice field in Eq. (1) by

$$u_n(t) \equiv (-1)^n \tilde{u}_n^*(t), \quad (7)$$

where the asterisk stands for complex conjugate [16]. The substitution reverses the sign of the nonlinearity in the respective equation for \tilde{u}_n into self-focusing:

$$i \frac{d\tilde{u}_n}{dz} = - (C_{n-1,n} \tilde{u}_{n-1} + C_{n,n+1} \tilde{u}_{n+1}) + (-1 + i\kappa_n) |\tilde{u}_n|^2 \tilde{u}_n, \quad (8)$$

hence it can support bright solitons pinned to the defect carrying the gain and loss. This possibility may be clarified in an analytical form, by considering a continuum counterpart of Eq. (8), with discrete coordinate n replaced by a continuous one, x , and a local defect of the coupling constant represented by term $\varepsilon \delta(x) |d\tilde{u}(x)/dx|^2$ in the respective Hamiltonian density, with $\varepsilon \sim C_d - C_0$, see Eq. (2), where $\delta(x)$ is the delta-function. With a localized shape of a bright soliton, $\tilde{u}_{\text{sol}}(x - \xi)$, whose center is placed at $x = \xi$, this term gives rise to the effective potential for the soliton,

$$U(\xi) = \varepsilon \left| \frac{d\tilde{u}_{\text{sol}}(\xi)}{d\xi} \right|^2. \quad (9)$$

In particular, the usual bright-soliton shape, $\tilde{u}_{\text{bright}} = A \operatorname{sech}(a\xi)$, with constants A and a , Eq. (9) yields

$$U_{\text{bright}}(\xi) = \varepsilon A^2 a^2 \sinh^2(a\xi) \operatorname{sech}^4(a\xi), \quad (10)$$

which features a potential minimum at $\xi = 0$ for $\varepsilon > 0$ and $\varepsilon < 0$, respectively. Thus, the defect is attractive at $\varepsilon > 0$, and repulsive at $\varepsilon < 0$. Incidentally, this argument explains the fact, reported in Ref. [44], that, in the case of $C_d < C_0$, the pinned mode in the discrete system with the self-focusing nonlinearity present solely at the two central sites carrying the gain and loss, the pinned mode exists above a finite threshold value of the total power (3).

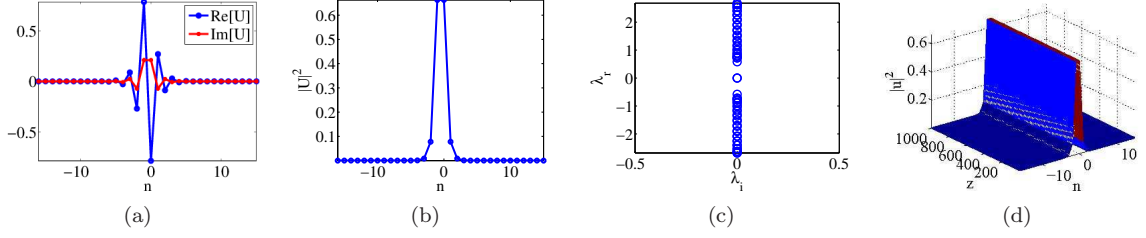


FIG. 2: (Color online) A typical example of a stable bright staggered soliton in the model based on Eq. (1), with $(P, C_d/C_0, \kappa) = (1.5, 2, 0.5)$. (a) Real (blue) and imaginary (red) parts of the solution. (b) The intensity profile of the soliton. (c) The spectrum of stability eigenvalues (which demonstrates that this soliton is stable). (d) Direct simulations of its perturbed evolution.

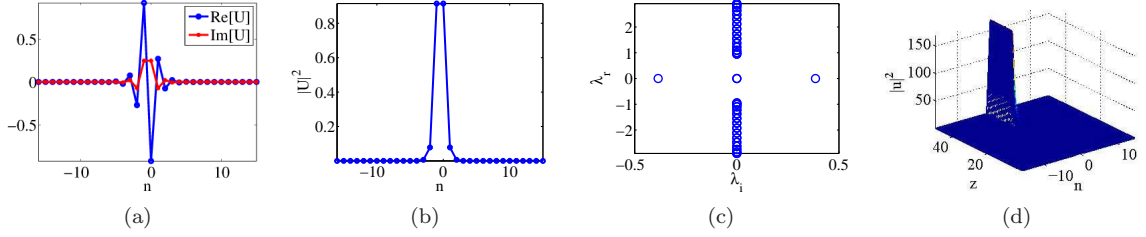


FIG. 3: (Color online) The same as in the previous figure, but for an unstable staggered soliton, with $(P, C_d/C_0, \kappa) = (2, 2, 0.5)$.

Indeed, in this case the defect repels the solitary mode, which must be compensated by the attraction induced by the nonlinearity concentrated at the central sites, while in the opposite case, $C_d > C_0$, there is no threshold.

Typical examples of stable and unstable staggered DSs, pinned to the \mathcal{PT} -symmetric defect, are displayed in Figs. 2 and 3, respectively. These figures clearly show that the real and imaginary parts of the wave field are indeed staggered (the real and imaginary parts are, severally, odd and even with respect to the midpoint between $n = -1$ and $n = 0$), while the intensity profile (the squared absolute value of the field) does not exhibit any staggering. Direct simulations demonstrate that the unstable DS undergoes a blowup under the action of the defect.

The results for the bright DSs of this type are summarized in stability charts in parameter planes of (κ, P) and $(\kappa, C_d/C_0)$, which are displayed in Fig. 4 [recall that P is the total power defined by Eq. (3)]. The figure demonstrates that the pinned bright DS gains stability with the increase of the intrinsic coupling strength of the dimer, C_d , while the increase of the the gain-loss coefficient, κ , naturally leads to destabilization. Indeed, larger values of C_d make the pinning potential (9) stronger, and also facilitate maintaining the balance between the gain and loss, while larger κ make this harder. It is also seen that there is no minimum (threshold) value of P necessary for the existence of the staggered bright DSs.

B. Unstaggered bright modes

Uniform nonlinear waveguide arrays with self-defocusing nonlinearity cannot support unstaggered bright DSs. However, unstaggered localized modes may exist, being pinned to the attractive defect. The numerical solution of Eq. (1) produces such modes, see an example in Fig. 5. They all are *stable*, their existence areas in the planes of $(\kappa, C_d/C_0)$ and $(P, C_d/C_0)$ being displayed in Fig. 6. Similar to the staggered DS, the increase of the intrinsic coupling constant of the dimer, C_d , helps to expand the existence area of the bright modes, which starts from $C_d/C_0 = 1$, see Fig. 6(b). Note also that, as well as the staggered modes considered above, the unstaggered ones exhibit no finite existence threshold in terms of the total power, as seen in Figs. 6(b,c).

In dependences of the propagation constant on the total power, displayed in Fig. 6(c), attaining the level of $d\mu/dP = 0$ (designated by horizontal dashed lines) implies a transition to delocalized states. Actually, these are anti-gray modes considered below.

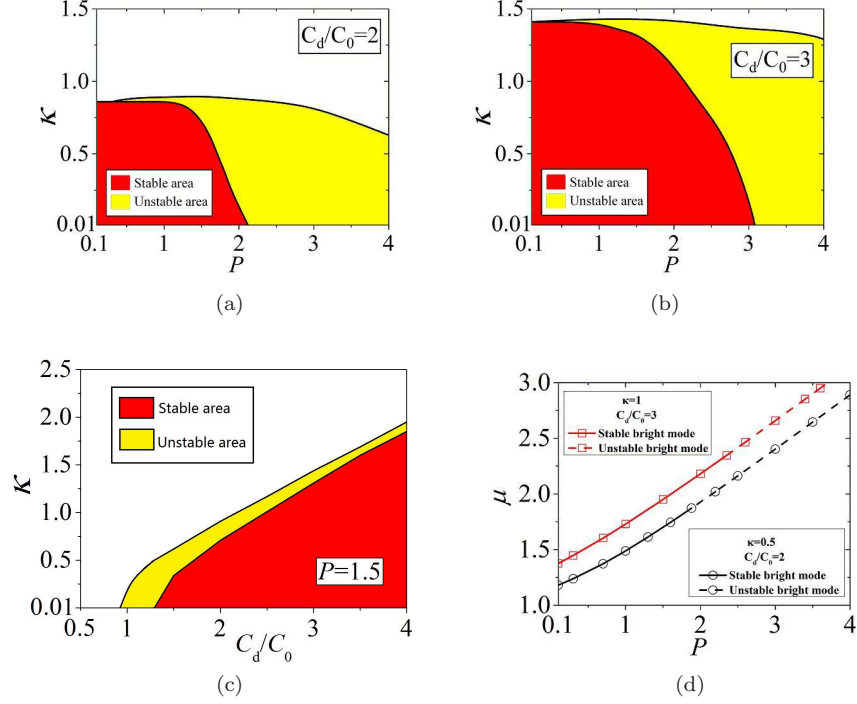


FIG. 4: (Color online) Existence regions of stable and unstable bright staggered solitons in the model based on Eq. (1) in the planes (κ, P) with $C_d/C_0 = 2$ (a) and $C_d/C_0 = 3$ (b). (c) The stability diagram in the $(\kappa, C_d/C_0)$ plane with $P = 1.5$. The solitons are stable and unstable, respectively, in red and yellow areas. No staggered bright solitons have been found in white areas. (d) Dependence of $\mu(P)$ for the stagger solitons at fixed values of other parameters.

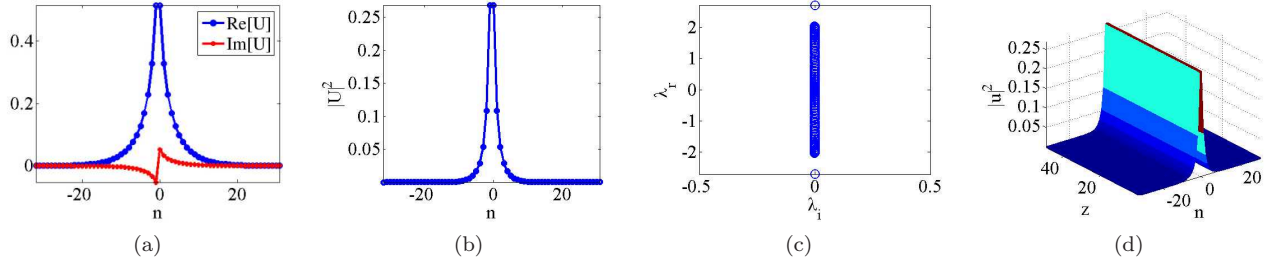


FIG. 5: (Color online) A typical example of a bright unstaggered mode produced by Eq. (1) for $(P, C_d/C_0, \kappa) = (1, 2, 0.1)$. Panels have the same meaning as in Fig. 2.

IV. GRAY AND ANTI-GRAY DISCRETE SOLITONS

A. Comparison with the continuum-model counterpart

Gray DSs are solutions to Eq. (1) supported by the nonzero background intensity, $|U_{BG}|^2$, which, in turn, is linked to the propagation constant by an obvious relation:

$$|U_{BG}|^2 = \mu + 2C_0. \quad (11)$$

The interaction of gray solitons with the defect may be estimated, in the continuum limit, by means of the effective potential (9), where a dark-soliton solution should be substituted. For a typical shape of this solution, $u_{\text{dark}} = A \tanh(a\xi)$, Eq. (9) yields

$$U_{\text{dark}}(\xi) = \varepsilon A^2 a^2 \text{sech}^4(a\xi). \quad (12)$$

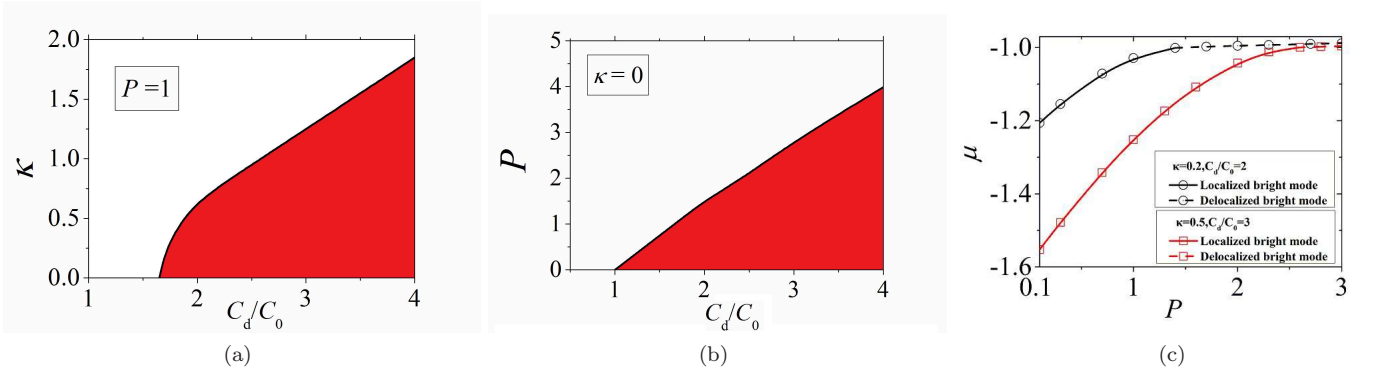


FIG. 6: (Color online) The existence area (red) of the unstaggered bright modes (which are all stable) in the plane of $(\kappa, C_d/C_0)$ (here $P = 1$ is fixed) (a), and $(P, C_d/C_0)$ (here $\kappa = 0$ is fixed) (b). In the white area, solutions are delocalized. (c) Dependences $\mu(P)$ for the modes.

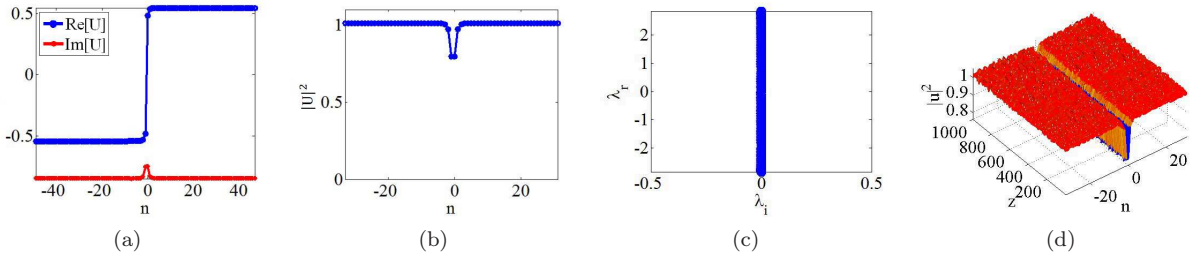


FIG. 7: (Color online) A typical example of a stable gray soliton produced by Eq. (1) with $(|U_{BG}|^2, C_d/C_0, \kappa) = (1, 1.1, 0.5)$. Panels have the same meaning as in Fig. 2.

On the contrary to its counterpart for the bright soliton, given by Eq. (10), this potential features a maximum at $\xi = 0$ for $\varepsilon > 0$, and a minimum for $\varepsilon < 0$, hence it may be expected to be attractive in the latter case, which, as said above, corresponds to $C_d < C_0$. Indeed, at strengths of the gain and loss, κ , small enough, stable gray solitons pinned to the defect tend to exist at $C_d/C_0 < 1$, as can be seen below in Fig. 9(b).

As said above, anti-gray solitons feature elevation on top of the finite background, rather than the dip characteristic to the gray ones. The estimate based on using the effective potential (9) is not relevant for them, as free anti-gray solitons do not exist in the continuum limit. In fact, the numerical results presented below reveal their existence, in the form pinned to the defect in the discrete system, at $C_d > C_0$ [see Fig. 9(b)], which would correspond to $\varepsilon > 0$ in the continuum limit. On the other hand, it is shown below that the existence of the anti-gray solitons pinned to the defect can be explained by means of another (strongly discrete) analytical approximation, see Eqs. (14)-17).

B. Numerical results

To find solutions of the gray and anti-gray types, we used the imaginary-time-propagation method, fixing the total power as $P = 128$, which is exactly equal to the total number of the lattice sites, $N = 128$. If we neglect a relatively small effect of the soliton's core and boundary conditions on P , the corresponding background level is $|U_{BG}|^2 \approx P/N = 1$, which makes it nearly fixed for the gray and anti-gray DSs.

The numerical analysis has demonstrated that both the gray and anti-gray DSs, pinned to the \mathcal{PT} -dimer defect, are *completely stable* whenever they exist. The gray DS, supported by the finite background, has a dip at the center, with a non-zero minimum value, while the anti-gray DS features a central hump on top of the background. Typical examples of stable DSs of both types are displayed in Figs. 7 and 8.

The solitons of these types are characterized by the “grayness degree”,

$$\Xi = \frac{|U_{n=-1}|^2 + |U_{n=0}|^2}{2|U_{BG}|^2} \quad (13)$$

where $|U_{BG}|^2$ is the background intensity, given by Eq. (11). Values $\Xi < 1$ and $\Xi > 1$ imply that the DS is gray or

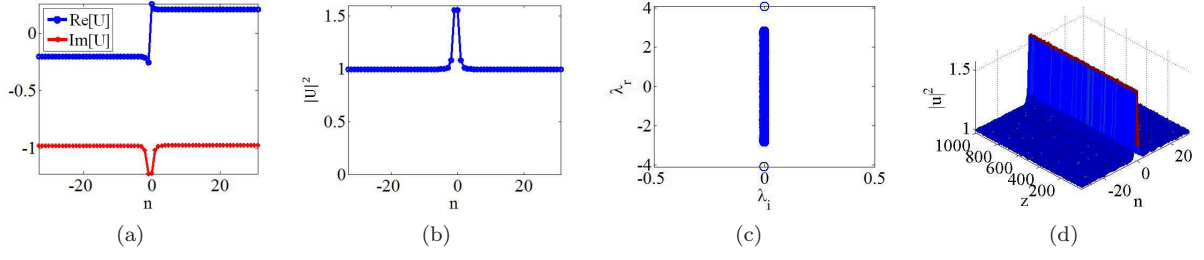


FIG. 8: (Color online) A typical example of a stable anti-gray soliton produced by Eq. (1), with $(|U_{\text{BG}}|^2, C_d/C_0, \kappa) = (1, 2.5, 0.5)$. Panels have the same meaning as in Fig. 2.

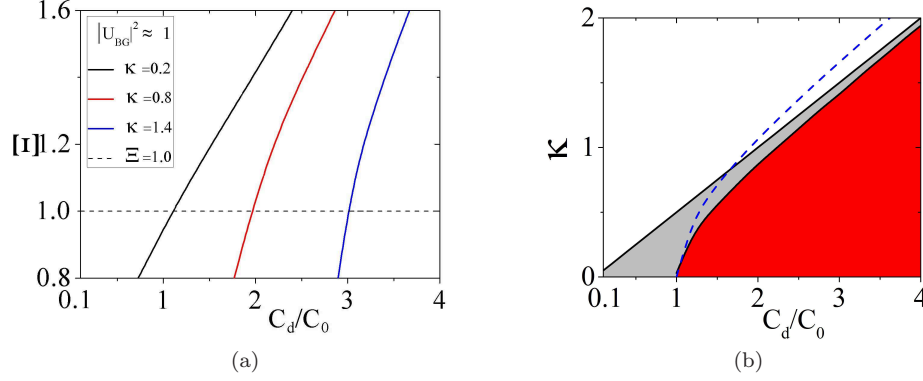


FIG. 9: (Color online) (a) The grayness degree, which is defined in Eq. (13), as a function of the dimer's intrinsic coupling constant, C_d . The plot comprises both the gray and anti-gray discrete solitons. The dashed line labels $\Xi = 1$. (b) Existence regions of stable gray and anti-gray discrete solitons (the gray and red areas, respectively) in the (κ, P) plane. In the white area, no soliton solutions were found. Here we fix $P = 128$, which corresponds to the background intensity $|U_{\text{BG}}|^2 \approx 1$, see the text. The dashed blue curve in (b) depicts the analytical approximation given by Eq. (17).

anti-gray, respectively, while $\Xi \equiv 1$ implies a flat state, which is a border between them. Figure 9(a) displays Ξ vs. C_d/C_0 at different fixed values of κ .

Stability regions of the gray and anti-gray solitons in the $(\kappa, C_d/C_0)$ plane are displayed in Fig. 9(b). This figure shows that the boundary between them, $\Xi = 1$ [see Eq. (13)], exactly coincides with $C_d/C_0 = 1$ when $\kappa = 0$ (the gain and loss are absent), which is explained by the fact that the conservative defect is attractive at $C_d/C_0 > 1$, and repulsive at $C_d/C_0 < 1$. The same argument explains the observation that, at $\kappa > 0$, the increase of C_d/C_0 leads to the expansion of the existence region for the anti-gray DSs, and shrinkage of that for the gray solitons.

C. An analytical approximation for the discrete system

The overall existence boundary for the DSs in Fig. 9(b) is exactly $\kappa = C_d$. This feature is explained by the well-known fact that the \mathcal{PT} symmetry of the dimer is broken at $\kappa > C_d$ [57, 62, 64]. As shown in Ref. [44], the same boundary remains relevant when the dimer is embedded into a linear lattice.

The boundary between the gray and anti-gray DSs in Fig. 9(b) can be predicted in an approximate analytical form. Indeed, it follows from Eq. (13) that condition $\Xi = 1$ implies that $|U_n| \equiv |U_{\text{BG}}|$, which suggests to approximate the respective solution by ansatz

$$U_n = \begin{cases} |U_{\text{BG}}|, & \text{at } n < -1 \text{ and } n > 0, \\ |U_{\text{BG}}|e^{-i\delta/2}, & \text{at } n = -1, \\ |U_{\text{BG}}|e^{+i\delta/2}, & \text{at } n = 0. \end{cases} \quad (14)$$

The substitution of this ansatz, along with relation (11), into Eq. (1), and looking at it solely at the defect-carrying

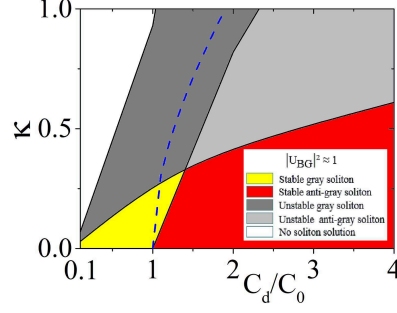


FIG. 10: (Color online) Stability regions (yellow and red) of gray and anti-gray solitons in the $(\kappa, C_d/C_0)$ plane, at $|U_{BG}|^2 \approx 1$ (the approximate equality is understood here in the same sense as before, i.e., $P = 128$ for the system built of $N = 128$ sites). In dark and light gray areas, respectively, unstable gray and anti-gray solitons have been found. In the white area, no soliton solutions exist. The dashed blue curve depicts the analytical approximation (17) for the boundary between gray and anti-gray solitons.

sites, $n = -1$ and $n = 0$, leads to an equation for δ and κ ,

$$C_d e^{-i\delta/2} + C_0 - 2C_0 e^{i\delta/2} + i\kappa e^{i\delta/2} = 0, \quad (15)$$

the solution of which is

$$\delta = 2 \arctan \left(\frac{\kappa}{2C_0 + C_d} \right), \quad (16)$$

$$\kappa^2 = \frac{1}{2} \left[\sqrt{C_0^4 + 8C_0^2 C_d^2 + 16C_0^3 C_d - (7C_0^2 - 2C_d^2)} \right]. \quad (17)$$

In the limit of $C_d \rightarrow \infty$, Eq. (17) simplifies to $\kappa \approx C_d$. The blue dashed curve in Fig. 9(b) displays relation (17), demonstrating that it produces a reasonable, although not very accurate, approximation.

D. Gray and anti-gray discrete solitons in the system with the nonlinear \mathcal{PT} symmetry

For bright DS modes, both staggered and unstaggered ones, the consideration of the model based on Eq. (6) with the defect carrying the nonlinear \mathcal{PT} symmetry (NPTS) produces results which are not qualitatively different from those reported above for its linear- \mathcal{PT} -symmetry counterpart, therefore we do not discuss them in detail here. However, new features appear in the NPTS system for gray and anti-gray DSs: while, as shown above, they are completely stable in the case of the dimer with the linear \mathcal{PT} symmetry, the NPTS version generates a nontrivial boundary in the parameter space between stable and unstable solitons of these types. These results are summarized in Fig. 10.

The analytical result for the model with the linear \mathcal{PT} -symmetric dimer, represented by Eq. (17), can be easily generalized for the NPTS system, replacing κ in those results by $\kappa|U_{BG}|^2$, pursuant to Eqs. (6) and (2). In particular, for the latter system with $|U_{BG}|^2 = 1$, which is represented by Fig. 10, the boundary between the areas of gray and anti-gray DSs is approximated by the same equation (17) as above, which is shown by the blue dashed curve in Fig. 10.

As seen in Fig. 10, the increase of the dimer's intrinsic coupling constant, C_d , stabilizes the DSs, while the increase of the gain-loss coefficient, κ destabilizes them, as before. However, the dynamics of unstable gray and anti-gray DSs is different from the blowup, which was observed for unstable staggered bright DSs [see Fig. 3(d)]: as shown in Figs. 11 and 12, the instability initiates internal oscillations in the solitons, and intensive emission of waves propagating on top of the stable background.

V. CONCLUSION

The objective of this work was to extend the variety of dynamical lattices with \mathcal{PT} -symmetric defects, by introducing the system with the background defocusing nonlinearity. In addition to the system with the defect in the form of

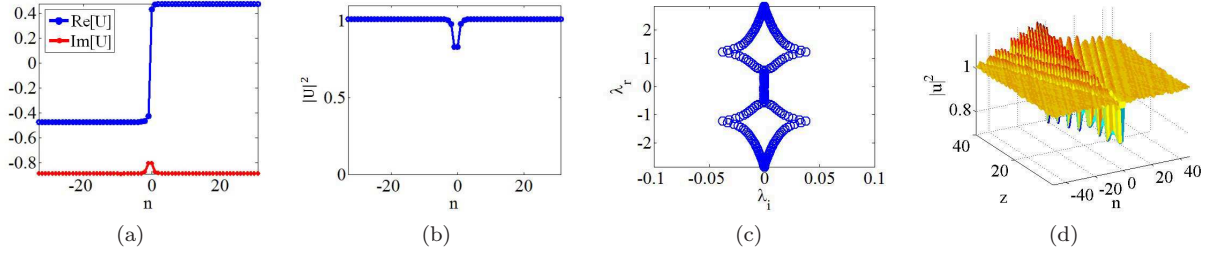


FIG. 11: (Color online) A typical example of an unstable gray soliton with $(|U_{BG}|^2, C_d/C_0, \kappa) = (1, 1, 0.5)$ in the model with the nonlinear \mathcal{PT} symmetry of the embedded dimer, based on Eq. (6). The panels have the same meaning as in Fig. 2.

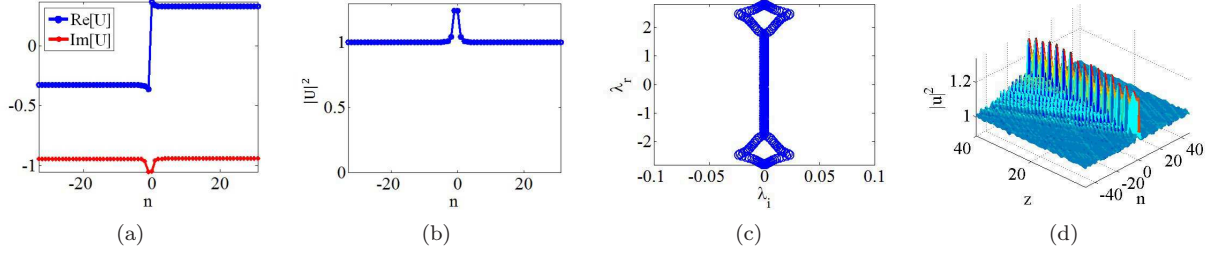


FIG. 12: (Color online) The same as in Fig. 11, but for an unstable anti-gray soliton with $(|U_{BG}|^2, C_d/C_0, \kappa) = (1, 2, 0.5)$.

the dimer with the linear \mathcal{PT} symmetry, a modification with the nonlinear \mathcal{PT} symmetry was considered too. The systems can be realized as arrays of optical waveguides with evanescent coupling. In comparison with the recently introduced model with the \mathcal{PT} -symmetric dimer embedded into a linear lattice [44], the new system gives rise to new types of DSs (discrete solitons), namely staggered and unstaggered bright ones, and gray and anti-gray DSs, depending on the relative strength of the dimer's intrinsic coupling constant, C_d . The existence of staggered bright and (unstaggered) gray can be explained in a qualitative form, with the help of the continuum limit. The boundary between gray and anti-gray DSs has been predicted too, in an approximate analytical form. Stability of the modes was investigated through the computation of the growth rates for small perturbations, and by means of direct simulations. The existence and stability areas tend to expand with the increase of C_d , and shrink with the increase of the gain-loss coefficient, κ . In particular, the bright unstaggered modes pinned to the defect are completely stable. The gray and anti-gray DSs are completely stable too in the system with the linear \mathcal{PT} symmetry of the defect, and have a boundary between stable and unstable states in the case of the nonlinear \mathcal{PT} symmetry. In the latter case, unstable DSs do not blow up, which is typical for unstable solitons in \mathcal{PT} -symmetric systems; instead, they develop oscillatory dynamics.

It may be interesting to consider DSs in the self-defocusing lattice with a pair of defects of the same or opposite signs (dimer-dimer, or dimer-antidimer), separated by some distance. A challenging perspective for the extension of the present analysis is to carry it out for the two-dimensional variant of the models. In that case, the \mathcal{PT} -symmetric defect may be represented by a dimer or quadrimer, and gray and anti-gray DSs will be, probably, replaced by vortices.

Acknowledgments

The authors appreciate useful discussions with Dr. Wei Pang (Guangdong University of Technology). This work is supported by the National Natural Science Foundation of China (Grants 11104083 and 11204089). B.A.M. appreciates hospitality of the Sun Yat Sen University (Guangzhou).

-
- [1] S. Aubry, "Breathers in nonlinear lattices: Existence, linear stability and quantization", *Physica D* **103**, 201-250 (1997).
 - [2] S. Flach and C. R. Willis, "Discrete breathers", *Phys. Rep.* **295**, 181-264 (1998).
 - [3] O. M. Braun and Y. S. Kivshar, "Nonlinear dynamics of the Frenkel-Kontorova model", *Phys. Rep.* **306**, 1-108 (1998).

- [4] C. M. Bender, D.C. Brody, and H. F. Jones, "Complex Extension of Quantum Mechanics", Phys. Rev. Lett. **89**, 270401 (2002); C. M. Bender, "Must a Hamiltonian be Hermitian?", Am. J. Phys. **71**, 1095 (2003); Z. Ahmed, "Real and complex discrete eigenvalues in an exactly solvable one-dimensional complex PT-invariant potential", Phys. Lett. A **282**, 343 (2001).
- [5] A. Trombettoni and A. Smerzi, "Discrete Solitons and Breathers with Dilute Bose-Einstein Condensates", Phys. Rev. Lett. **86**, 2353 (2001).
- [6] S. Lepri, R. Livi, and A. Politi, "Thermal conduction in classical low-dimensional lattices", Phys. Rep. **377**, 1-80 (2003).
- [7] E. Laermann and O. Philipsen, "Lattice QCD at finite temperature", Ann. Rev. Nucl. Part. Sci. **53**, 163-198 (2003).
- [8] D. N. Christodoulides, F. Lederer, and Y. Silberberg, "Discretizing light behaviour in linear and nonlinear waveguide lattices", Nature **424**, 817 (2003).
- [9] M. A. Porter, R. Carretero-González, P. G. Kevrekidis, and B. A. Malomed, "Nonlinear lattice dynamics of Bose-Einstein condensates", Chaos **15**, 015115 (2005).
- [10] M. Sato, B. E. Hubbard, and A. J. Sievers, "Nonlinear energy localization and its manipulation in micromechanical oscillator arrays", Rev. Mod. Phys. **78**, 137-157 (2006).
- [11] K. G. Makris, R. El-Ganainy, D. N. Christodoulides, and Z. H. Musslimani, "Beam Dynamics in PT Symmetric Optical Lattices", Phys. Rev. Lett. **100**, 103904 (2008).
- [12] S. Flach and A. V. Gorbach, "Discrete breather-Advances in theory and applications", Phys. Rep. **467**, 1 (2008).
- [13] F. Lederer, G. I. Stegeman, D. N. Christodoulides, G. Assanto, M. Segev, and Y. Silberberg, "Discrete solitons in optics", Phys. Rep. **463**, 1 (2008).
- [14] D. J. Frantzeskakis, "Small-amplitude solitary structures for an extended nonlinear Schrödinger equation", J. Phys. A: Math. Gen. **29**, 3639 (1996).
- [15] JOURNAL OF PHYSICS A-MATHEMATICAL AND GENERAL Volume: 29 Issue: 13 Pages: 3631-3639 Published: JUL 7 1996
- [16] P. G. Kevrekidis, "The Discrete Nonlinear Schrödinger Equation: Mathematical Analysis", Numerical Computations, and Physical Perspectives (Springer: Berlin and Heidelberg, 2009).
- [17] Y. V. Kartashov, V. A. Vysloukh and L. Torner, "Soliton shape and mobility control in optical lattices", Progr. Optics **52**, 63-147 (2009).
- [18] U. Röpke, H. Bartelt, S. Unger, K. Schuster, and J. Kobelke, "Fiber waveguide arrays as model system for discrete optics", Appl. Phys. B **104**, 481-486 (2011).
- [19] F. Eilenberger, S. Minardi, A. Szameit, U. Röpke, J. Kobelke, K. Schuster, H. Bartelt, S. Nolte, A. Tünnermann, and T. Pertsch, "Light bullets in waveguide arrays: spacetime-coupling, spectral symmetry breaking and superluminal decay [Invited]", Opt. Exp. **19**, 23171-23187 (2011).
- [20] G. Colangelo, S. Durr, A. Jüttner, L. Lellouch, H. Leutwyler, V. Lubicz, S. Necco, C. T. Sachrajda, S. Simula, A. Vladikas, U. Wenger, and H. Wittig, "Review of lattice results concerning low-energy particle physics", Eur. Phys. J. C **71**, 1695 (2011).
- [21] I. L. Garanovich, S. Longhi, A. A. Sukhorukov, and Y. S. Kivshar, "Light propagation and localization in modulated photonic lattices and waveguides", Phys. Rep. **518**, 1-79 (2012).
- [22] R. Lifshitz, E. Kenig, and M. C. Cross, "Collective dynamics in arrays of coupled nonlinear resonators", in: *Fluctuating Nonlinear Oscillators*, ed. by M. I. Dykman (Oxford University Press, Oxford, 2012), Chapter 11.
- [23] D. N. Christodoulides, E. D. Eugenieva, "Blocking and routing discrete solitons in two-dimensional networks of nonlinear-waveguides arrays", Phys. Rev. Lett. **87**, 233901 (2001); D. N. Christodoulides, E. D. Eugenieva, "Minimizing bending losses in two-dimensional discrete soliton networks", Opt. Lett. **26**, 1876 (2001); E. D. Eugenieva, N. K. Efremidis, and D. N. Christodoulides, "Design of switching junctions for two-dimensional discrete soliton networks", Opt. Lett. **26**, 1978 (2001).
- [24] T. Hattori, N. Tsurumachi, and H. Nakatsuka, "Analysis of optical nonlinearity by defect states in one-dimensional photonic crystals", J. Opt. Soc. Am. B **14**, 348 (1997).
- [25] Y. Akahane, T. Asano, B. S. Song, and S. Noda, "High-Q photonic nanocavity in a two-dimensional photonic crystal", Nature **425**, 944 (2003).
- [26] R. Colombelli, K. Srinivasan, M. Troccoli, O. Painter, C. F. Gmachl, D. M. Tennant, A. M. Sergent, D. L. Sivco, A. Y. Cho, and F. Capasso, "Quantum cascade surface-emitting photonic crystal laser", Science **302**, 1374 (2003).
- [27] H. Nakamura, Y. Sugimoto, K. Kanamoto, N. Ikeda, Y. Tanaka, Y. Nakamura, S. Ohkouchi, Y. Watanabe, K. Inoue, H. Ishikawa, and K. Asakawa, "Ultra-fast photonic crystal/ quantum dot all-optical switch for future photonic networks", Opt. Express **12**, 6606 (2004).
- [28] X. D. Cao and B. A. Malomed, "Soliton-defect collisions in the nonlinear Schrödinger equation", Phys. Lett. A **206**, 177-182 (1995).
- [29] U. Peschel, R. Morandotti, J. S. Aitchison, H. S. Eisenberg, and Y. Silberberg, "Nonlinearly induced escape from a defect state in waveguide arrays", Appl. Phys. Lett. **75**, 1348 (1999); R. Morandotti, H. S. Eisenberg, D. Mandelik, Y. Silberberg, D. Modotto, M. Sorel, C. R. Stanley, and J. S. Aitchison, "Interactions of discrete solitons with structural defects", Opt. Lett. **28**, 834 (2003).
- [30] F. Fedele, J. Yang, and Z. Chen, "Defect modes in 1D photonic lattices", Opt. Lett. **30**, 1506 (2005); L. Morales-Molina and R. A. Vicencio, "Trapping of discrete solitons by defects in nonlinear waveguide arrays", Opt. Lett. **31**, 966 (2006); X. Wang, J. Young, Z. Chen, D. Weinstein, and J. Yang, "Observation of lower to higher bandgap transition of one-dimensional defect modes", Opt. Exp. **14**, 7362 (2006).
- [31] B. Freedman, G. Bartal, M. Segev, R. Lifshitz, D. N. Christodoulides and J. W. Fleischer, "Wave and defect dynamics in

- nonlinear photonic quasicrystals”, *Nature* **440**, 1166 (2006).
- [32] Y. S. Kivshar, M. I. Molina, “Nonlinear localized modes at phase-slip defects in waveguide arrays”, *Opt. Lett.* **33**, 917 (2008).
 - [33] Y. Li, W. Pang, Y. Chen, Z. Yu, J. Zhou, and H. Zhang, “Defect-mediated discrete solitons in optically induced photorefractive lattices”, *Phys. Rev. A* **80**, 043824 (2009); X. Zhang, J. Chai, D. Ou, and Y. Li, “Antisymmetry breaking of discrete dipole gap solitons induced by a phase-slip defect”, *Mod. Phys. Lett. B* **28**, 1450097 (2014); J. Huang, H. Li, X. Zhang, Y. Li, “Transmission, reflection, scattering, and trapping of traveling discrete solitons by \mathcal{C} and \mathcal{V} point defects”, *Front. Phys.* **10**, 104201 (2015).
 - [34] M. I. Molina and G. Tsironis, “Nonlinear impurities in a linear chain,” *Phys. Rev. B* **47**, 15330 (1993).
 - [35] B. C. Gupta and K. Kundu, “Formation of stationary localized states due to nonlinear impurities using the discrete nonlinear Schrödinger equation,” *Phys. Rev. B* **55**, 894 (1997).
 - [36] B. C. Gupta and K. Kundu, “Stationary localized states due to a nonlinear dimeric impurity embedded in a perfect one-dimensional chain”, *Phys. Rev. B* **55**, 11033 (1997).
 - [37] B. Maes, M. Soljačić, J. D. Joannopoulos, P. Bienstman, R. Baets, S.-P. Gorza, and M. Haelterman, “Switching through symmetry breaking in coupled nonlinear micro-cavities,” *Opt. Exp.* **14**, 10678-10683 (2006).
 - [38] E. N. Bulgakov and A. F. Sadreev, “Bound states in photonic Fabry-Perot resonator with nonlinear off-channel defects,” *Phys. Rev. B* **81**, 115128 (2010).
 - [39] E. Bulgakov, A. Sadreev, and K. N. Pichugin, “Symmetry breaking for transmission in a photonic waveguide coupled with two off-channel nonlinear defects,” *Phys. Rev. B* **83**, 045109 (2011).
 - [40] V. A. Brazhnyi and B. A. Malomed, “Spontaneous symmetry breaking in Schrödinger lattices with two nonlinear sites”, *Phys. Rev. A* **83**, 053844 (2011).
 - [41] V. A. Brazhnyi and B. A. Malomed, “Localization and delocalization of two-dimensional discrete solitons pinned to linear and nonlinear defects”, *Phys. Rev. E* **83**, 016604 (2011).
 - [42] A. E. Miroshnichenko, B. A. Malomed, and Y. S. Kivshar, “Nonlinearly \mathcal{PT} -symmetric systems: Spontaneous symmetry breaking and transmission resonances”, *Phys. Rev. A* **84**, 012123 (2011).
 - [43] S. V. Dmitriev, S. V. Suchkov, A. A. Sukhorukov, and Y. S. Kivshar, “Scattering of linear and nonlinear waves in a waveguide array with a \mathcal{PT} -symmetric defect,” *Phys. Rev. A* **84**, 013833 (2011); S. V. Suchkov, A. A. Sukhorukov, S. V. Dmitriev, and Y. S. Kivshar, “Scattering of the discrete solitons on the \mathcal{PT} -symmetric defects”, *Europhys. Lett.* **100**, 54003 (2012).
 - [44] X. Zhang, J. Chai, J. Huang, Z. Chen, Y. Li, and B. A. Malomed, “Discrete solitons and scattering of lattice wave in guiding arrays with a nonlinear \mathcal{PT} -symmetric defect,” *Opt. Exp.* **22**, 13927 (2014).
 - [45] Z. Chen, J. Liu, S. Fu, Y. Li, and B. A. Malomed, “Discrete solitons and vortices on two-dimensional lattices of \mathcal{PT} -symmetric couplers”, *Opt. Exp.* **22**, 29679 (2014).
 - [46] B. A. Malomed, E. Ding, K. W. Chow and S. K. Lai, “Pinned modes in lossy lattices with local gain and nonlinearity”, *Phys. Rev. E* **86**, 036608 (2012).
 - [47] K. W. Chow, E. Ding, B. A. Malomed, and A. Y. S. Tang, “Symmetric and antisymmetric nonlinear modes supported by dual local gain in lossy lattices”, *Eur. Phys. J. Special Topics* **223**, 63-77 (2014).
 - [48] E. Ding, A. Y. S. Tang, K. W. Chow, and B. A. Malomed, “Pinned modes in two-dimensional lossy lattices with local gain and nonlinearity”, *Phil. Trans. Roy. Soc. A* **372**, 20140018 (2014).
 - [49] T. Mayteevarunyoo, B. A. Malomed, and A. Roeksabutr, “A solvable model for solitons pinned to a \mathcal{PT} -symmetric dipole”, *Phys. Rev. E* **88**, 022919 (2013); N. Karjanto, W. Hanif, B. A. Malomed, and H. Susanto, “Interactions of bright and dark solitons with localized \mathcal{PT} -symmetric potentials”, *Chaos* **25**, 023112 (2015).
 - [50] A. Ruschhaupt, F. Delgado, and J. G. Muga, “Physical realization of \mathcal{PT} -symmetric potential scattering in a planar slab waveguide,” *J. Phys. A* **38**, L171-L176 (2005).
 - [51] K. G. Makris, R. El-Ganainy, D. N. Christodoulides, and Z. H. Musslimani, “Beam dynamics in \mathcal{PT} symmetric optical lattices,” *Phys. Rev. Lett.* **100**, 103904 (2008).
 - [52] S. Longhi, “Spectral singularities and Bragg scattering in complex crystals,” *Phys. Rev. A* **81**, 022102 (2010).
 - [53] H. Ramezani, T. Kottos, R. El-Ganainy, and D. N. Christodoulides, “Unidirectional nonlinear \mathcal{PT} -symmetric optical structures”, *Phys. Rev. A* **82**, 043803 (2010).
 - [54] S. Longhi, “Invisibility in \mathcal{PT} -symmetric complex crystals”, *J. Phys. A: Math. Theor.* **44**, 485302 (2011).
 - [55] K. G. Makris, R. El-Ganainy, D. N. Christodoulides, and Z. H. Musslimani, “ \mathcal{PT} symmetric periodic optical potentials,” *Int. J. Theor. Phys.* **50**, 1019-1041 (2011).
 - [56] Y. V. Kartashov, B. A. Malomed, and L. Torner, “Unbreakable \mathcal{PT} symmetry of solitons supported by inhomogeneous defocusing nonlinearity”, *Opt. Lett.* **39**, 5641-5644 (2014).
 - [57] D. A. Zezyulin and V. V. Konotop, “Nonlinear modes in finite-dimensional \mathcal{PT} -symmetric systems,” *Phys. Rev. Lett.* **108**, 213906 (2012).
 - [58] C. E. Rüter, K. G. Makris, R. El-Ganainy, D. N. Christodoulides, M. Segev, and D. Kip, “Observation of parity-time symmetry in optics,” *Nature Phys.* **6**, 192-195 (2010).
 - [59] Z. Lin, J. Schindler, F. M. Ellis, and T. Kottos, “Experimental observation of the dual behavior of \mathcal{PT} -symmetric scattering,” *Phys. Rev. A* **85**, 050101 (2012).
 - [60] A. Regensburger, M. A. Miri, C. Bersch, and J. Näger, “Observation of defect states in \mathcal{PT} -symmetric optical lattices,” *Phys. Rev. Lett.* **110**, 223902 (2013).
 - [61] I. V. Barashenkov, G. S. Jackson, and S. Flach, “Blow-up regimes in the \mathcal{PT} -symmetric coupler and the actively coupled dimer,” *Phys. Rev. A* **88**, 053817 (2013).

- [62] J. Pickton and H. Susanto, “Integrability of \mathcal{PT} -symmetric dimers,” *Phys. Rev. A* **88**, 063840 (2013).
- [63] A. S. Rodrigues, K. Li, V. Achilleos, P. G. Kevrekidis, D. J. Frantzeskakis, and C. M. Bender, “ \mathcal{PT} -symmetric double-well potentials revisited: bifurcations, stability and dynamics”, *Rom. Rep. Phys.* **65**, 5 (2013).
- [64] K. Li, P. G. Kevrekidis, and B. A. Malomed, “Nonlinear modes and symmetries in linearly-coupled pairs of \mathcal{PT} -invariant dimers”, *Stud. Appl. Math.* **133**, 281-297 (2014).
- [65] K. Li, D. A. Zezyulin, P. G. Kevrekidis, V. V. Konotop, and F. K. Abdullaev, “ \mathcal{PT} -symmetric coupler with $\chi^{(2)}$ nonlinearity,” *Phys. Rev. A* **88**, 053820 (2013).
- [66] F. Kh. Abdullaev, Y. V. Kartashov, V. V. Konotop, and D. A. Zezyulin, “Solitons in \mathcal{PT} -symmetric nonlinear lattices”, *Phys. Rev. A* **83**, 041805(R) (2011); D. A. Zezyulin, Y. V. Kartashov and V. V. Konotop, “Stability of localized modes in \mathcal{PT} -symmetric nonlinear potentials”, *EPL* **96**, 64003 (2011).
- [67] K. Staliūnas and V. J. Sánchez-Morcillo, “Transverse Patterns in Nonlinear Optical Resonators”, *Springer Tracts in Modern Physics*, Vol. 183 (Springer-Verlag, Berlin, 2003). .
- [68] M. L. Chiofalo, S. Succi, and M. P. Tosi, “Ground state of trapped interacting Bose-Einstein condensates by an explicit imaginary-time algorithm “, *Phys. Rev. E* **62**, 7438 (2000).
- [69] G. P. Agrawal, *Applications of Nonlinear Fiber Optics* (Academic Press: San Diego, 2001).
- [70] H. Li, Z. Shi, X. Jiang, and X. Zhu, “ Gray solitons in parity-time symmetric potentials,” *Opt. Lett.* **36**, 3290 (2011).